Journal of Fluids and Structures (2002) **16**(1), 113–119
doi:10.1006/jfls.2001.0414, available online at http://www.idealibrary.com on IDEAL®

NEURAL NETWORK CONTROL OF VORTEX SHEDDING FROM A CIRCULAR CYLINDER USING ROTATIONAL FEEDBACK OSCILLATIONS

N. Fujisawa
Department of Mechanical and Production Engineering, Niigata University 8050 Ikarashi 2, Niigata, 950-2181, Japan

AND

T. Nakabayashi
Department of Mechanical Engineering, Gunma University, 1-5-1 Tenjin Kiryu, 376-8515, Japan

(Received 26 July 2000, and in final form 29 May 2001)

The performance of active control of vortex shedding from a circular cylinder is studied experimentally with rotational feedback oscillations. The optimization of the control parameters, such as the phase lag, the feedback gain, and the position of reference sensor are carried out using neural networks to minimize the reference velocity fluctuations in the cylinder wake. Measurement of pressure distributions over the circular cylinder under the optimum control indicate that the drag force is reduced by 16% and the lift force is suppressed by more than 70% in comparison with the stationary cylinder.

1. INTRODUCTION

The vortex shedding from a bluff-body structure in a stream has been a topic of interest for many years. Among the research work in the literature, the control of vortex shedding is very important from the practical point of view, because vortex shedding is closely related to the occurrence of flow induced vibrations and noise. Hence, various types of control are introduced for the attenuation of the vortex shedding from bluff-body structures. These results are summarized in review papers by Bearman (1984), Griffin & Hall (1991), and so on.

The feedback control of vortex shedding was first introduced by Ffowcs Williams & Zhao (1989) and this control strategy was applied to various problems in thermal and fluid engineering. Very recently, the effect of feedback control on the fluid force on the cylinder was examined experimentally by Fujisawa *et al.* (2001). In this experiment, the feedback signal was obtained from the velocity fluctuation in the cylinder wake and was fed back into the rotational oscillation of the cylinder. The drag force was reduced by 11% by this control, when the control parameters, such as phase lag and feedback gain, are selected optimally. However, the optimum combinations of these parameters are expected to change with variations of the reference sensor position. Hence, the automatic optimization of these parameters is important for the control and further reduction of the fluid forces acting on the circular cylinder.

The objective of the present paper is to investigate automatic optimization procedures for determining the control parameters in the feedback controls. A neural network is applied

0889–9746/02/010113 + 7 $35.00/0

for this purpose and the optimum aerodynamic performance of the circular cylinder under feedback control is evaluated by measuring the pressure distributions around the circular cylinder.

2. EXPERIMENTAL APPARATUS AND PROCEDURE

2.1. Experimental Apparatus

The experiments are carried out in a low-speed wind tunnel with a square test-section of $0{\cdot}5\,\mathrm{m} \times 0{\cdot}5\,\mathrm{m}$ and $1{\cdot}5\,\mathrm{m}$ long providing a uniform flow velocity. A circular cylinder of a diameter $D = 100\,\mathrm{mm}$ is positioned horizontally at the center of the open test-section and supported by two vertical side walls, spanning the axis normal to the flow direction. The experiments are carried out at free-stream velocity $U = 3\,\mathrm{m/s}$, which corresponds to a Reynolds number Re $(= DU/\nu) = 2 \times 10^4$. Two hot-wires are positioned in the cylinder wake; one is a reference sensor for feedback control and the other is a monitor sensor for measuring the velocity fluctuations in a typical position of the cylinder wake in response to the control. The position of the monitor sensor is fixed at $(x/D = 1{\cdot}5,\ y/D = 0{\cdot}8)$ in the present experiment. Here, x is a distance from the cylinder center along the free stream, y is that in the vertical direction perpendicular to the free stream. These hot-wire sensors are made from tungsten wire 5 μm in diameter and 1 mm in length. The velocity fluctuation (u_r) at the reference sensor in the cylinder wake is processed through a linearizer, a high-pass filter at 1·6 Hz and a low-pass filter at 6·6 Hz. The filtered velocity (u_{rf}) is transmitted to a microcomputer fitted with AD and DA converter and supplied to the AC servo motor, which provides a rotational oscillation to the circular cylinder up to a frequency of 8 Hz. The phase lag ϕ between the angular velocity signal of the motor and the feedback velocity signal and the feedback gain $\alpha(= R\omega_{\max}/u_{rf\max})$ are set in digital in the computer, where $\omega_{\max}$ is a maximum angular velocity of the cylinder and $u_{rf\max}$ is a maximum of the filtered velocity. Further details of the experimental apparatus, including the validity of the experiment and feedback control loop, are described by Fujisawa *et al.* (2001).

2.2. Neural Network Model

The optimization of the control parameters such as the phase lag and the feedback gain are carried out using a neural network, which automatically outputs the optimum parameters after suitable learning. Figure 1 shows an illustration of a neural network model used in the present study, which consists of three layers of neurons with back-propagation algorithms.

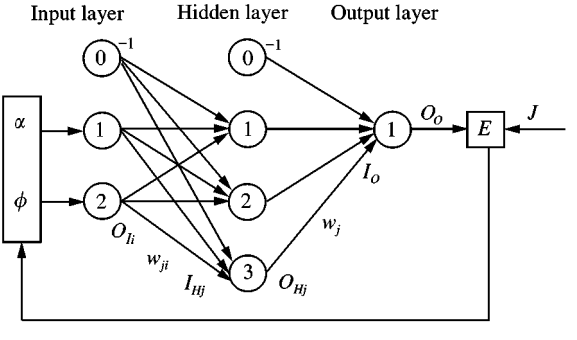

Figure 1. Neural network model.

There are two units at the input layer, three units at the hidden layer, and one unit at the output layer. The phase lag ϕ and the feedback gain α are used as input parameters. When these input parameters are abbreviated by I_i ($I_1 = \alpha$, $I_2 = \phi$), the output of the input layer O_{Ii} can be described as follows:

$$O_{Ii} = 1/(1 + \exp(-I_i/T_I)). \tag{1}$$

The relations between the input I_{Hj} and output O_{Hj} at the hidden layer of the neural network model are described as follows:

$$I_{Hj} = \sum w_{ji} I_j - w_{10}, \qquad O_{Hj} = 1/(1 + \exp(-I_{Hj}/T_H)), \tag{2, 3}$$

where w_{ji} is a weight between the input and hidden layer. Similarly, the total input I_O and output O_O at the output layer are given as follows:

$$I_O = \sum w_j O_{Hj} - w_{20}, \qquad O_O = 1/(1 + \exp(-I_O/T_O)), \tag{4, 5}$$

where w_j is a weight between the hidden and output layer. The introduction of the neuron temperatures T_I, T_H, T_O in the sigmoidal functions is known to reduce the learning error and hence the CPU time (Mastsuura 1997). The number of units at the hidden layer and the neuron temperatures are determined from the point of learning error and CPU time, which are conducted before starting the learning by the neural network model. The weights w_{ji} and w_j are given by some random values in the initial phase of learning. When the actual learning of the neural network starts, not only the weights w_{ji}, w_j but also the input parameters are modified by the steepest descent method to minimize the learning error $E = (J - O_O)^2/2$, where J is an evaluation function (Li & Nagaya 1997). It is to be noted that the modification of the input parameters is carried out only when the learning of the neural network has finished after the iteration cycle of 5000, which was found to be large enough for the training of neural network model. Then, the learning of the neural network starts again with the new input parameters and the trained weights, which again outputs the new input parameters. This procedure is continued until the velocity fluctuations become as small as possible.

For the application of this neural network model to the present study, the evaluation function is set to $J = \int_0^T u_r'^2 \, dt$, where u_r' is the velocity fluctuations at the reference sensor, t is the time, and T is the integration time. The selection of the integration time T is important to reach a convergence of the optimization. When the integration time T is set to a value less than 20 wavelengths, the output parameters vary largely with time, which may be due to the unsteadiness of the velocity fluctuations in the cylinder wake. It is found that an increase in the integration time stabilizes the output, but it needs more computing time, which results in a poor response of the control system to the disturbances. Therefore, the integration time is set to a rather short wavelength number of 7 and the evaluation function is averaged over previous five sets of functions. This procedure improves both the convergence and the response of the optimization.

3. RESULTS AND DISCUSSIONS

3.1. Optimization of Control Parameters

Figure 2(a–c) shows a typical example of the response of the cylinder wake to the neural network control using rotational feedback oscillation. The variations of streamwise velocity fluctuations at the monitor sensor are plotted against the time t after the start of control in Figure 2(a), and the corresponding time variations of the phase lag ϕ and feedback gain α are given in Figure 2(b,c), respectively. Here, the reference sensor for control is set to

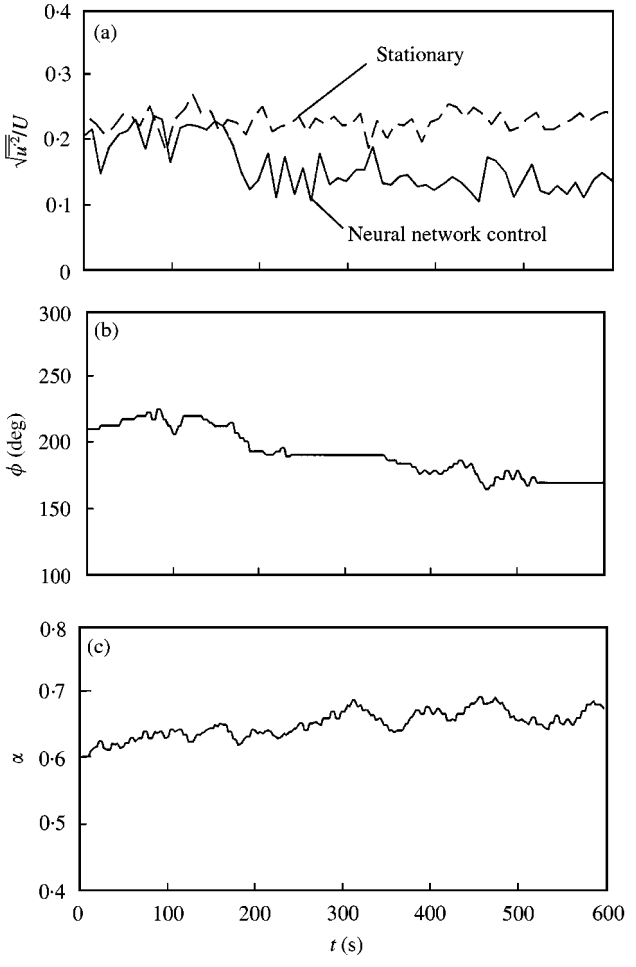

Figure 2. Time variations of monitored velocity fluctuations and control parameters under feedback control using neural network: (a) velocity fluctuations; (b) phase lag; (c) feedback gain.

position ($x/D = 2$, $y/R = -1{\cdot}2$) in the shear layer. The control effect can be recognized in the traces of velocity fluctuations in Figure 2(a) after $t = 180$ s. of the start of neural network control, where the reference velocity fluctuations under the control become smaller than those of the stationary cylinder. Hereafter, the control effect is saturated and reaches a steady state. Corresponding to the reduction in velocity fluctuations, the phase lag ϕ decreases from the initial value and the corresponding feedback coefficient α increases gradually as shown in Figure 2(b,c), respectively. The time variations of the control parameters are waving slowly, which may be due to the large velocity fluctuations in the cylinder wake.

Figure 3(a–c) shows the distributions of streamwise velocity fluctuations at the monitor sensor for various positions of reference probe in (a), the corresponding distributions of phase lag in (b), and the feedback gain in (c). It is noted that the coordinates x, y in Figure 3 indicate the position of the reference sensor and the values in the figure correspond to the velocity fluctuations at the monitor sensor. The results are obtained by applying the present optimizations to 35 points of the reference sensor in the cylinder wake ranging $x/D = 0$–3

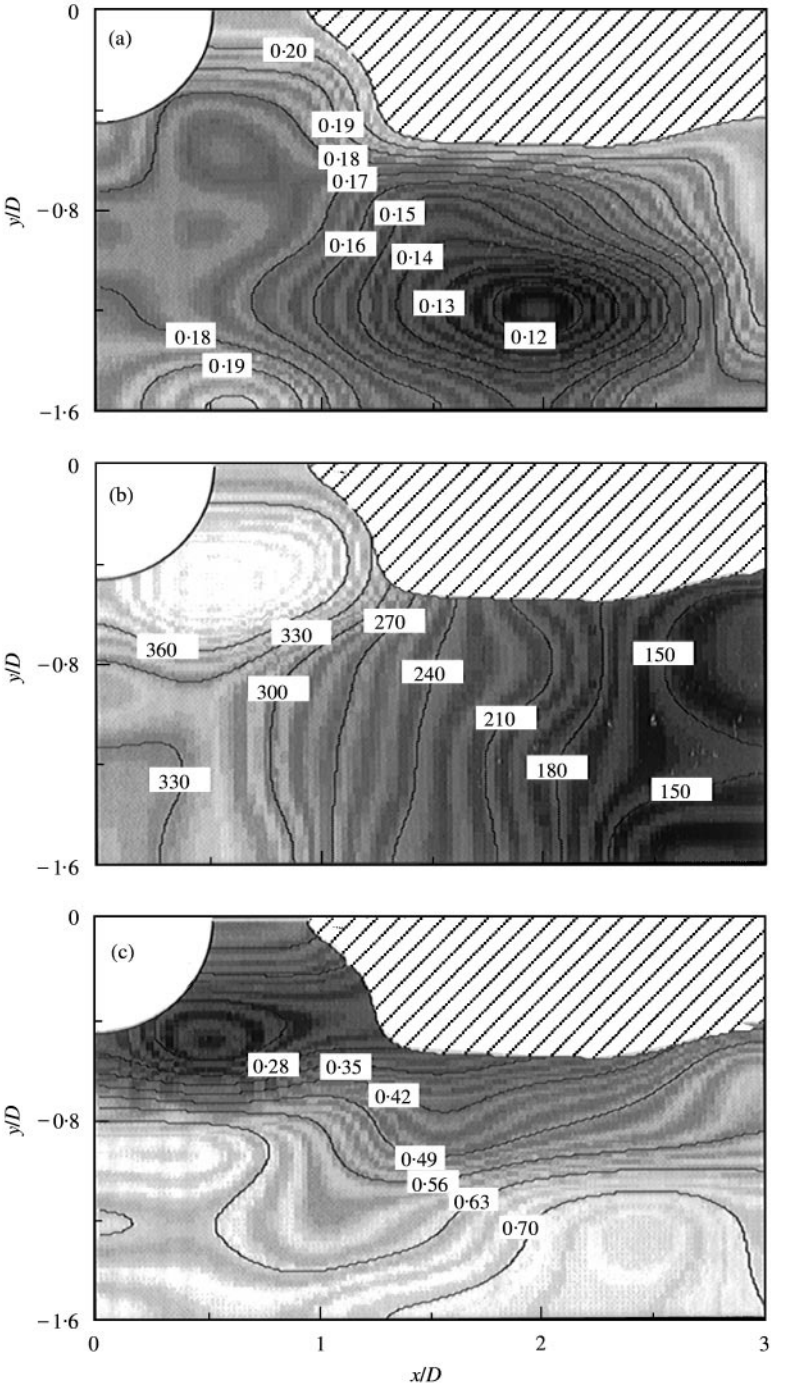

Figure 3. Distributions of monitored velocity fluctuations and control parameters at various positions of reference sensor: (a) monitored velocity fluctuations; (b) phase lag; (c) feedback gain.

and $y/D = -1{\cdot}5$–0. It can be seen from Figure 3(a) that the monitored velocity fluctuations become smallest when the reference sensor is located around the optimum position ($x/D = 2$, $y/D = -1{\cdot}2$). The region of smaller velocity fluctuations extends from the

cylinder side, downstream along the shear layer. However, the optimization study with neural networks was not successful in the shaded area behind the cylinder, where the variations of velocity fluctuations with respect to the control parameters are very small. It is expected that the gradient type law used in the steepest descent method of neural networks will not be applicable to such an area to obtain a suitable local minimum. According to Figure 3(b,c), the optimum phase lag at the optimum reference-sensor-position is found to be around $\phi = 180^\circ$, and the corresponding optimum feedback gain is about $\alpha = 0{\cdot}7$. The optimum phase lag decreases as the reference sensor moves downstream and the optimum feedback gain increases as the reference sensor moves outside the cylinder, which indicates the influence of the convection velocity of the shear layer separating from the cylinder and the distribution of velocity fluctuations in the cylinder wake, respectively.

3.2. Fluid Force Characteristics

Figure 4 shows the phase averaged drag and lift coefficient $C_{d\theta}(= 2F_x/\rho U^2 D)$, $C_{l\theta}(= 2F_y/\rho U^2 D)$ of the circular cylinder under the feedback control and those of the stationary cylinder, which are plotted against the phase angle ψ of vortex shedding. Here, F_x and F_y are streamwise and normal fluid forces acting on the cylinder, respectively. The uncertainty interval of the measurement is estimated to be $\pm$ 5% at 95% coverage. It is to be noted that the natural frequency of vortex shedding for the present stationary cylinder was observed at a Strouhal number of 0·2 and the time-averaged drag coefficient was found to be 1·08 (Fujisawa *et al.* 1998), which were in close agreement with the results in the

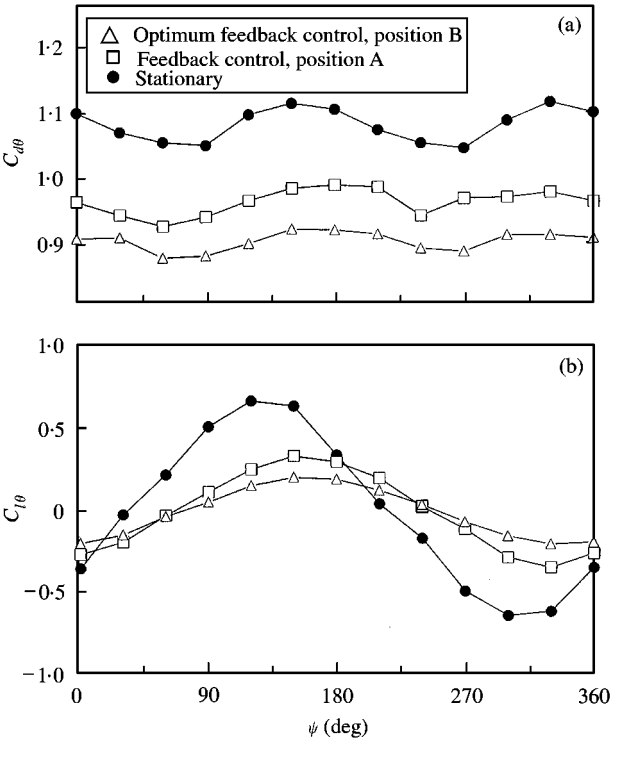

Figure 4. Phase-averaged drag and lift coefficient in relation to phase angle of vortex shedding: (a) drag coefficient; (b) lift coefficient.

literature (King 1977). Two control results at different reference-sensor position are shown in this figure: one is for the feedback sensor at position A ($x/D = 1{\cdot}5$, $y/D = -0{\cdot}8$) and the other is at the optimum feedback sensor position B ($x/D = 2$, $y/D = -1{\cdot}2$). It is clearly seen that the aerodynamic performance of the cylinder is improved by the control, in comparison with the stationary cylinder. Better control efficiency appears on the aerodynamic performance when the feedback sensor is located at the optimum position B than that at position A, reflecting the reduction in the velocity fluctuations at the reference sensor, as observed in Figure 3. It should be mentioned that the maximum reduction in the phase-averaged drag coefficient is 16% and that in the lift coefficient is over 70% in comparison with the stationary cylinder. These results indicate an improvement in the aerodynamic performance of the cylinder under feedback control, by optimizing the control parameters and feedback sensor position suggesting the usefulness of the present neural network optimization procedures. However, the drag reduction observed here is much smaller than those measured by Tokumaru (1991) with a simple rotational oscillation of the cylinder, which reaches 80% in drag reduction at the peak rotation rate of 2 and at several times larger forcing frequency of cylinder oscillation than the natural one. The observed difference in the drag reduction may be due to the dominant frequency of the feedback signal used in the present study, which is fixed at the vortex shedding frequency. Further study will be useful for the determination of forcing frequency in the feedback control and the use of the transverse velocity component for the feedback signal, which is known to be a more robust indicator of the intensity of vortex shedding.

4. CONCLUSIONS

The performance of active control of vortex shedding from a circular cylinder by rotational feedback oscillation is studied experimentally using neural networks. The proposed neural network model with back propagation algorithm is successfully applied to the optimization study of control parameters, such as the phase lag and the feedback gain, to obtain an optimum performance of the feedback controls. The optimum position of the reference sensor is found to be distributed along the shear layer, and the most effective position for attenuating the vortex shedding is found to be at $x/D = 2$ and $y/D = -1.2$. The drag force is reduced by 16% and the lift force is suppressed more than 70% under the optimum feedback control in comparison with the stationary cylinder.

REFERENCES

BEARMAN, P. W. 1984 Vortex shedding from oscillating bluff bodies. *Annual Review of Fluid Mechanics* **16,** 195–222.

FFOWCS WILLIAMS, J. E. & ZHAO, B. C. 1989 The active control of vortex shedding. *Journal of Fluids and Structures* **3,** 115–122.

FUJISAWA, N., IKEMOTO, K. & NAGAYA, K. 1998 Vortex shedding resonance from a rotationally oscillating cylinder. *Journal of Fluids and Structures* **12,** 1041–1053.

FUJISAWA, N., KAWAJI, Y. & IKEMOTO, K. 2001 Feedback control of vortex shedding from a circular cylinder by rotational oscillations. *Journal of Fluids and Structures* **15,** 23–37.

GRIFFIN, M. & HALL, M. S. 1991 Review: Vortex shedding lock-in and flow control in bluff body wakes. *ASME Journal of Fluids Engineering* **113,** 526–537.

KING, R. 1977 A review of vortex shedding research and its application. *Ocean Engineering* **4,** 141–171.

LI, L. & NAGAYA, K. 1997 Control of sound noise radiated from a plate using dynamic absorbers under the optimization by neural network. *Journal of Sound and Vibration* **208,** 289–298.

MATSUURA, T. 1997 Adaptive control of flexible arms by neural network. *Proceedings of Japan Society of Mechanical Engineers*, Kiryu, 144–145.

TOKUMARU, P. T. & DIMOTAKIS, P. E. 1991 Rotary oscillation control of a cylinder wake. *Journal of Fluid Mechanics* **224,** 77–90.